ILASS 2008
Sep. 8-10, 2008, Como Lake, Italy

Paper ID ILASS08-13-9

AN EXPERIMENTAL STUDY OF SPRAY/WALL INTERACTION FOR HEATED, WETTED SURFACES

Monika Mühlbauer*, Feras Z. Batarseh°, Bodo Durst*, Ilia V. Roisman°, Markus Selder*, Cameron Tropea°

*BMW AG, Hufelandstr. 4, 80788 Munich, Germany, monika.muehlbauer@bmw.de
° Chair of Fluid Mechanics and Aerodynamics, Darmstadt University of Technology,
Petersenstr. 30, 64287 Darmstadt, Germany, roisman@sla.tu-darmstadt.de

ABSTRACT
The concept of direct injection (DI) is often applied in modern spark-ignited engines. Thereby, the fuel is injected under high pressures of up to 200 bar into the combustion chamber. Before complete evaporation, interactions of spray drops with wall surfaces may occur. The spray/wall interaction under these conditions of high surface temperatures and surfaces partly covered with an oil film has rarely been studied yet and is therefore not well understood.
This motivated an experimental investigation using the phase Doppler technique (PDA). The convex target in form of a hemisphere of 2cm radius can be heated up to temperatures above 200°C and an only gravity-driven oil film can be established on the surface. A hollow cone spray with isooctane as fluid is used. The ambient pressure and temperature are restricted to atmospheric conditions. The setup and results of the experiment are discussed and the latter are also compared to the results according to the spray/wall interaction model of G. Elsässer [6] which is currently used in numerical simulations at BMW. As this model is based on single drop data, whereas the spray considered in this work is very dense, the influence of drop/drop interactions becomes apparent.

INTRODUCTION

The current development concerning spark-ignited engines often includes the concept of direct injection (DI) in order to fulfil the demands of high efficiency yet low emissions. The fuel spray is injected under a pressure of up to 200bar into the combustion chamber. Before completely evaporating, spray drops may collide with wall surfaces. The complex interaction phenomena are of major interest in the development of a DI engine in several respects:

- They influence thoroughly air/fuel mixing and hence the combustion process.
- The formation of a wall film leads to higher soot and HC emissions. These can be provoked, on the one hand, by diffusion flames burning the wall film. On the other hand, the inserted fuel may not immediately take part in the combustion process but only later when evaporating off the wall film during the exhaust stroke.
- On the cylinder running surface, an oil film exists which is decisive with respect to adequate lubrication of the piston movement. During spray/wall interaction, spray fluid can be added to this oil film which can result in critical oil dilution.

Conditions under which spray/wall interaction in an operating engine occur. Spray drops can hit various surface parts, including the piston, the cylinder running surface, the intake valves, or the spark plug. Depending on the load, the associated surface temperatures T_{Wall} and the ambient pressure $p_{ambient}$ vary quite significantly: at rated power, for instance, the intake valves can exhibit temperatures of up to 600 K at ambient pressures in an approximate range of 0.8 - 2.5 bar. At part load, impacts at ambient pressures of 0.3 – 1.2 bar may occur on the piston with a temperature below 400 K. Besides the variation of T_{Wall} and $p_{ambient}$, the coverage differs from surface to surface and can be quite different from a dry metallic surface with a defined roughness: The piston or the intake valves can be coked, i.e. covered by a rough and porous structure, whereas an oil film exists on the cylinder running surface.

Contents and aim of this work. To explain in-cylinder phenomena in an engine cycle, Computational Fluid Dynamics (CFD) is a valuable tool. For spray simulations, numerical codes often make use of an Euler-Lagrangian approach, i.e. physical particles are traced as a disperse phase in form of representative parcels. When a parcel hits a surface, the different interaction forces such as viscosity, surface tension etc. cannot be resolved in detail. Hence, the spray/wall interaction is rather defined by correlations between reflected and impacting diameters, velocity components and droplet numbers.

However, the reliability of numerical modelling of spray/wall interaction is very limited up to now due to the lack of appropriate models:

- Hardly any impact data have been measured under the wide parameter range occurring in an operating engine. Existing models can probably not be extrapolated to such conditions.
- Most existing models are based on single drop data which do not account for drop/drop interactions and the oscillating wall film flow. Comprehensive reviews of these models can be found in [1,2]. Yet, drop/drop interactions are proved to be more and more decisive [3]. In [4] it is shown that models, describing spray impact as a simple superposition of single drop impacts, cannot satisfactorily predict the impact of even a relatively sparse spray. The

complicated phenomena with respect to spray impact have been observed using a high-speed video system in [5].

Therefore, this work aims at providing experimental data to validate existing models and to build new models for the numerical treatment of spray/wall interaction at real in-cylinder conditions.

The phase Doppler technique (PDA) provides such data. A dual PDA setup is therefore used to measure diameters and two perpendicular velocity components in an experimental facility designed to operate at the relevant conditions.

It is hardly possible to vary all parameters which influence spray/wall interaction in a single experiment and the focus in this work lies on the surface temperature T_{Wall} and the surface coverage, particularly on the comparison between the impact on a dry and an oil-covered surface.

The chosen operating conditions will be presented in detail, followed by some short remarks about data evaluation and a discussion of the results. This includes a comparison of the results to those of the existing spray/wall interaction model of G. Elsässer [6], which is currently used in the development using CFD at BMW. It is based on various experimental data concerning single drop impact and includes extrapolations to the conditions under which spray/wall interactions occur in an operating engine. As the investigated spray is very dense, the comparison of the model outcome and the experimental data further reveals the importance of drop/drop interactions.

EXPERIMENTAL SETUP

Measurement technique. A dual PDA setup (λ_1 = 514.5 nm, λ_2 = 488 nm) is used to measure drop diameters and two perpendicular components of the velocity vector, U1 and V1, at the same time. In this experiment, scattered light of first-order refraction is observed under an off-axis angle of 30°.

Target design and wall film. As spray/wall interaction is of interest, the measuring points should lie as near to the surface as possible. The challenge to measure two perpendicular velocity components at such positions (each requires the intersection of two laser beams) dictates a target design in form of a hemisphere, see figure 1. Its radius is chosen as R_T = 2 cm and it resides on top of a cylinder with the same radius and 8 cm length. The target is made of copper and the surface is polished, resulting in a mean roughness of $R_a \approx 0.297$ µm.

Heating cartridges of altogether 3 000 W, which are mounted inside the target, allow the heating of the surface to very high temperatures in spite of spray cooling. The wall temperature, T_{Wall}, is measured at five different positions 2mm below the surface by thermocouples. The thermal expansion of the target has been studied by image subtraction and evaluation. Whereas the target radius R_T does not change remarkably, the vertical expansion cannot be neglected. To prevent associated adjustment errors in the measuring positions, the origin set in the target apex is readjusted at each new value of T_{Wall}.

Through a small tube of 2 mm diameter which ends at the target apex, an oil film can be established on the surface, see figure 2. An engine oil is chosen as film fluid. The film flow with constant volume flux, $\dot{Q}$, is driven solely by gravity. The resulting film thickness δ depends, amongst others, on the azimuthal position θ and can be estimated, for not too small values of θ, as:

$$\delta = \left(\frac{3}{2 \cdot \pi \cdot R_0 \cdot g} \cdot \upsilon \cdot \frac{\dot{Q}}{\sin^2 \theta} \right)^{1/3} . \qquad (1)$$

Two volume fluxes with values of

- $\dot{Q}_1 \approx 0.53$ ml/min and
- $\dot{Q}_2 \approx 1.1$ ml/min.

are used in the experiment.

The kinematic viscosity of the oil, ν, depends strongly on the temperature (the film temperature is assumed to be identical to T_{Wall}): $\nu(20°C) \approx 13.5 \times 10^{-5}$ m²/s, $\nu(150°C) \approx 0.43 \times 10^{-5}$ m²/s. This dependence transfers to the film thickness. Together with the two different values of the volume flux, this results at θ = 45°, for instance, in an approximate range from $\delta(\dot{Q}_1, 150°C) \approx 0.06$ mm to $\delta(\dot{Q}_2, 20°C) \approx 0.23$ mm.

Clearly, the studied values of δ are much larger than the film thickness on a cylinder running surface in an engine (typical value: δ ≈ 5 µm). However, much smaller volume fluxes can hardly be realized with the current film pump. Moreover, at low wall temperatures it is no longer possible to get a stable and continuous film surface on the target due to surface tension.

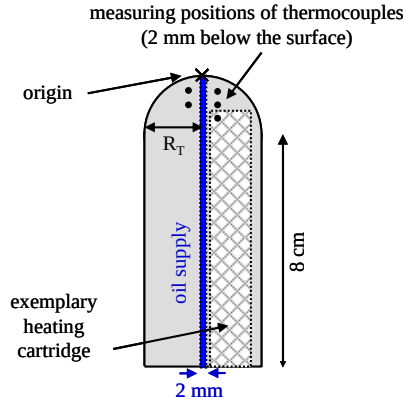

Fig. 1: Target design.

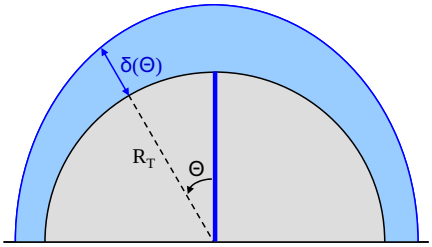

Fig.2: Sketch of an oil film on the target (exaggerated film depth for illustration).

Spray. A piezoelectric, outward-opening injector which produces a thin and very dense hollow-cone spray is used (injector ring gap ≈ 0.03 mm), see figure 3. The cone angle, determined by Mie scattering images, is 97.14°. The injection duration t_i and the time interval Δt_{SOI} between successive injections are adjustable. In order to get enough statistics, the

data of several injections must be summed up at each measuring point. Thereby, Δt_{SOI} must be chosen large enough to ensure that the original target surface is restored after the previous injection. This can lead to very large measuring times for one single measuring point (in case of an oil film at low T_{Wall} Δt_{SOI} >30 s, for example). Hence, to collect sufficient data in an acceptable time, t_i = 50 ms is chosen in the experiment, although this value is larger than in a normal engine cycle where t_i has an order of around 0.5 ms - 5 ms.

Isooctane at room temperature (≈ 25°C) is used as fuel.

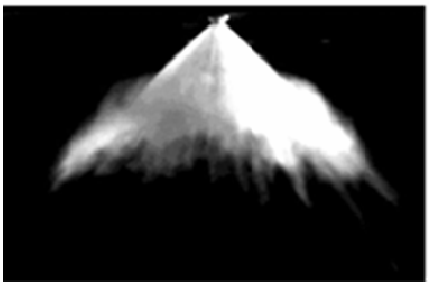

Fig.3: Mie scattering image of the spray.

Ambient conditions. Atmospheric conditions are chosen, i.e. an ambient pressure of $p_{ambient}$ ≈ 1 bar at room temperature.

Adjustment of target and injector. Figures 4 and 5 show the two relative positions between target and injector which are used in the experiment. They had to be manually adjusted, resulting in an estimated accuracy of ± 1mm. Target and spray axis define the measurement plane where all measurement points are situated.

Besides the measurement points themselves, both measured velocity components, U1 and V1, lie in the measurement plane, see figure 6. The third component normal to this plane is assumed to be zero due to the rotational symmetry of the studied dense spray.

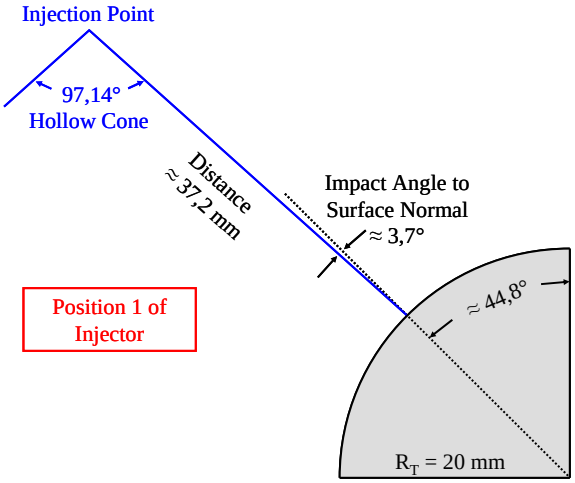

Fig.4: Relative position 1 between injector and target.

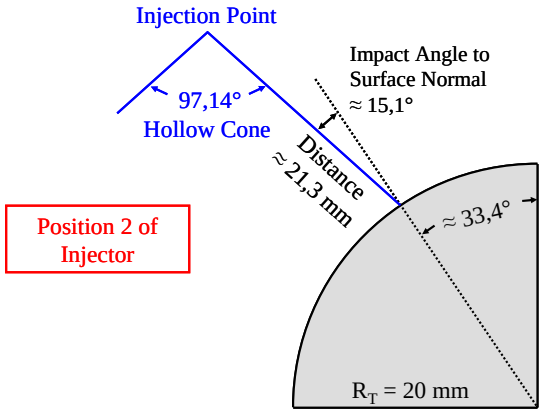

Fig.5: Relative position 2 between injector and target.

Locations of the measurement points. Figure 7 illustrates the grid used in each measurement (=one parameter setting) with dry target. Results associated with different distances from the target surface can be compared to study the influence of near-wall flow. In case of an oil film, the measurement points at a distance of 2 mm are not considered to ensure a sufficient distance from the wall film and from the coronas forming under drop impacts. Moreover, this saves measuring time which is a priori larger than for a dry target due to larger values of Δt_{SOI}.

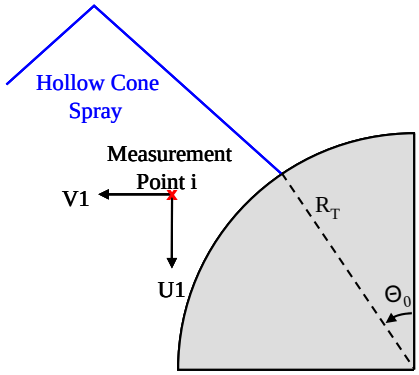

Fig.6: Measured velocity components U1, V1.

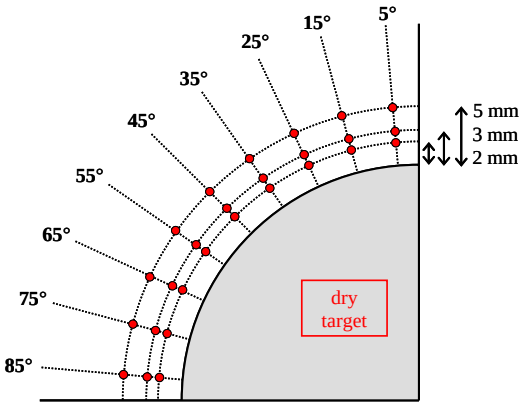

Fig.7: Grid of measurement points for a dry target.

Parameter variations in the experiment can be summarized as follows:

Wall temperature: T_{Wall} is varied from 20°C-200°C for a dry target surface. With an oil film on the target, the range is restricted to 20°C-150°C.

Surface coverage: The dry target as well as an oil covered target surface with two different volume fluxes of the oil fluid are considered: $\dot{Q}_1 \approx 0.53$ ml/min and $\dot{Q}_2 \approx 1.1$ ml/min.

Injection pressure and relative position between target and injector: Besides the main injection pressure of p_{Inj} = 50 bar, p_{Inj} = 150 bar is also considered for comparison of different incoming drop sizes and velocities. For the same reason, the position of the injector relative to the target has been varied, see figures 2 and 3. The order of magnitude of drop diameters and velocities are about 50 µm and 30 m/s respectively.

Due to the curvature of the target, a small variation in impact angles can also be studied.

DATA EVALUATION

For a study of spray/wall interaction, the wall normal and wall tangential velocity components, U2 and V2, are of interest. The coordinate system to which the measured data U1 and V1 refer is therefore not appropriate, see figure 6. However, it is not possible to adjust the optics in such a way as to measure directly U2 and V2 of each drop for all measuring points due to the curvature of the target and the small but finite width of the spray cone. Hence, careful data evaluation including several coordinate transformations has to be performed. Some essential questions must be addressed:

- The robustness and plausibility of the data have to be checked.
- A coordinate system tangential to the surface must be defined to which the wall normal and tangential velocity U2 and V2 of the drops are referred. Thereby, the distance between the measurement points (where information is collected) and surface (where information is desired) must be accounted for. Moreover, an interpolation between the discrete positions of the measurement points must be considered.
- Impacting (=primary) drops must be distinguished from reflected (=secondary) drops.
- The data must be transformed to be adapted to input and output quantities from numerical simulations.

Such basic issues are reflected in the following steps of the data processing:

- Each drop is projected from its measurement point along its velocity vector onto the target resulting in its individual wall contact point θ_{Con}. The position of the measurement point is then no longer of interest.
- At θ_{Con}, a local coordinate system normal and tangential to the surface is defined individually for each drop and its velocity components, U2 and V2, in this new coordinate system are calculated from the measured components, see figure 8. Note that the curvature of the dry target is used in defining the coordinate system even in cases of an oil film. The difference to the film surface has been calculated and estimated to be not decisive. Moreover, only the first impacting droplets find an undisturbed oil film surface. The state of the latter is not known for subsequent drops.
- If U2≥0, the drop is considered to be a primary (= incoming) drop, otherwise it is a secondary (= reflected) drop, see figure 9.

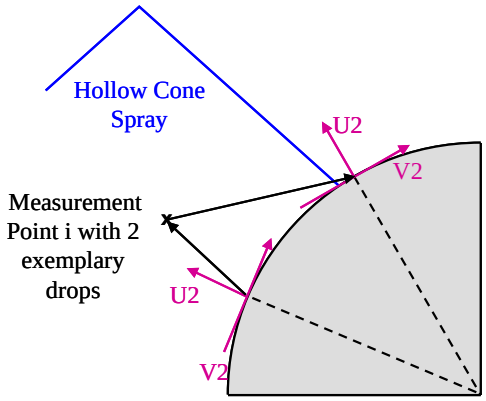

Fig.8: Projection of each drop onto the surface to determine its value θ_{Con} and definition of U2, V2.

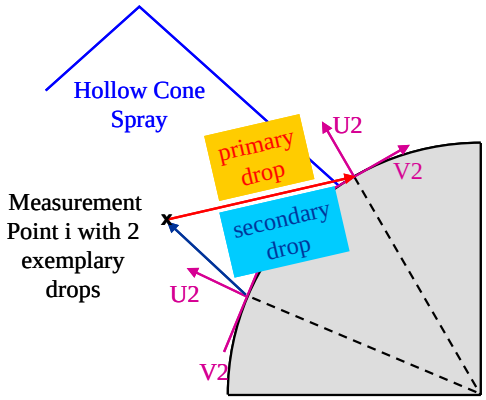

Fig.9: Distinction of primary and secondary drops.

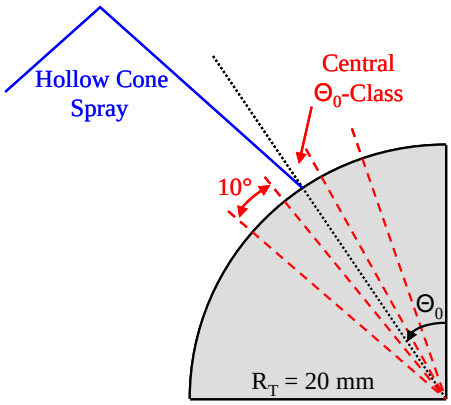

Fig.10: Definition of θ-classes on the surface.

- On the surface, θ-classes are established, see figure 10. The central class (maximal number of primary drops) is defined symmetrically around the central spray impact region. The other classes are grouped around the central class. They are equidistant and have a width of 10°. This value is chosen because the positions of the measurement points define the same spatial resolution. In final parameter variations only three classes, the central class, one on its left and one on its right are considered. The sample numbers associated to other classes which are even more distant from the central impact area are much smaller, leading to less reliable statistics.
- Due to the finite diameter d_t of the detection volume [7,8], θ_{Con} bears an uncertainty $\Delta\theta_{Con}$ (angle of the arc which is associated to the projection of d_t along the velocity vector of the drop onto the surface). The fraction

of the uncertainty band $\Delta\theta_{Con}$ which lies in each θ-class defines a weighting factor of the drop in the specific class.

- In each class weighted mean values and their standard deviations are determined for primary drops: $U2_{10,weighted,primary}$, $V2_{10,weighted,primary}$, $D_{10,weighted,primary}$ etc. Correction factors which account for multiple droplets in the detection volume at the same time are also included [7,8].
- In contrast to primary drops, secondary drops show bimodal distributions in their wall tangential velocity as expected, see figure 11. Therefore, they are split in the drops belonging to the mainly expected scattering direction (including forward scattering) and those of the so-called side scattering direction. The separation is drawn by the weighted mean impact angle of the primary drops in the respective class. It shows, that the reflection angle of each secondary mode is quite well defined, i.e. the associated distribution is characterized by a single and dominant peak.
- For each mode of secondary drops, weighted mean values and their standard deviations are calculated.
- Finally, transformations concerning the velocity components are performed to express the results independent of the target geometry and the θ-classes (which are of no interest in numerical modelling) and to adapt them to numerical input and output. Only the primary drops can then present the frame of reference. Therefore, their wall normal and tangential velocity components are set to positive values, the value of the diameter remains unchanged:

  $v_{N,primary} := |U2_{10,weighted,primary}|$,
  $v_{T,primary} := |V2_{10,weighted,primary}|$,
  $d_{primary} := |D_{10,weighted,primary}|$.

  The wall tangential component of the secondary drops must consequently be adapted to keep its sign relative to the primary drops:

  $v_{T,secondary} := sgn(V2_{10,weighted,secondary}/V2_{10,weighted,primary}) \cdot V2_{10,weighted,secondary}$.

  The wall normal velocity is still defined positively and other quantities are not changed either:

  $v_{N,secondary} := U2_{10,weighted,secondary}$.
  $d_{secondary} := D_{10,weighted,secondary}$
- For parameter variations, the weighted mean values d, v_N, v_T etc. of a specific θ-class (approximately same impact conditions) are compared, for example those of the central class. In the latter, results are most reliable due to the highest sample numbers.

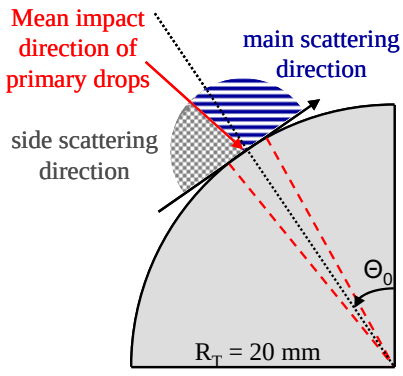

Fig.11: Splitting secondary drops into main and side scattering direction.

RESULTS

The presentation of the results has been restricted to the following exemplary cases:

- Data from measuring points with the minimal distance from the target are presented, see figure 7: For a dry target, this distance is 2 mm, for an oil-wetted surface 3 mm. The larger the distance the larger the assumed errors due to near-wall flow. The latter leads to an incorrect determination of θ_{Con} for each drop.
- Values of the central θ-class are shown.
- The values of v_N, v_T and d are compared. Information on impact / reflection angles and absolute velocities can be deduced from them. The evaluation of the mass fluxes which is of great interest but quite difficult (due to the point-like measuring technique interpolations must be conceived) has not yet been completed.
- The results of a representative variation in T_{Wall} temperature respectively in the surface coverage are presented. Further evaluations concerning the variation of the impacting drop sizes and velocities are not completely finished yet.

Wall temperature. The dependence of the impact outcome on T_{Wall} are shown exemplarily for a dry target in figures 12-14. The injection pressure is fixed to p_{Inj} = 50 bar and the relative position 1 between injector and target is chosen, see figure 4. The fact that the values associated with the primary drops remain approximately constant, confirms that the impact conditions are comparable for all values of T_{Wall}. The weighted mean impact angle (referred to the surface tangential) is 87.5° in this case. The impact is therefore nearly normal which implies that both directions of secondary drops are assumed to be equally important.

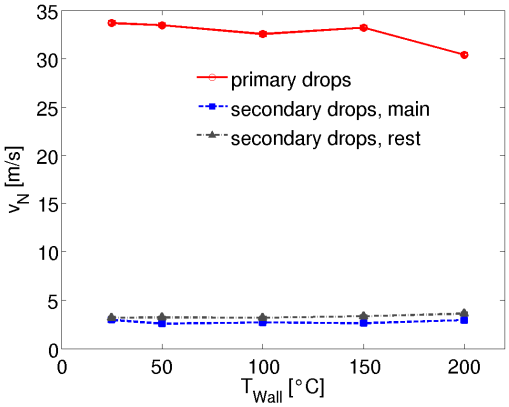

Fig.12: Dependence of wall normal velocity components v_N on the wall temperature T_{Wall} for a dry target with p_{Inj} = 50 bar and relative position 1 between injector and target.

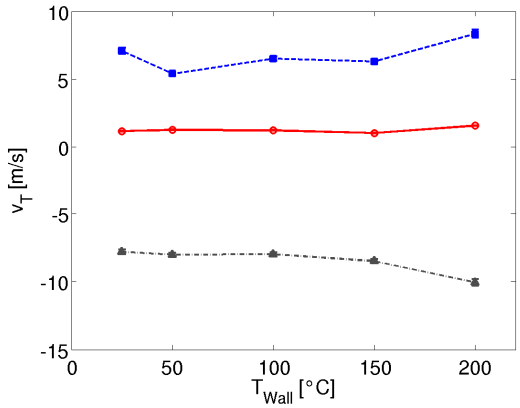

Fig.13: Dependence of wall tangential velocity components v_T on the wall temperature T_{Wall} for a dry target with p_{Inj} = 50 bar and relative position 1 between injector and target. Legend as in figure 12.

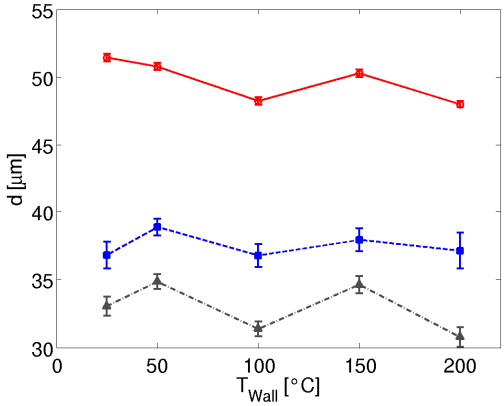

Fig.14: Average drop diameter d in dependence on the wall temperature T_{Wall} for a dry target with p_{Inj} = 50 bar and relative position 1 between injector and target. Legend as in figure 12.

Obviously, the influence of T_{Wall} is very small although the material properties of the liquids and the heat transfer change significantly in the considered range of T_{Wall}. According to single drop impact, no direct drop/wall contact beyond the Leidenfrost temperature should occur due to a vapor cushion forming between the drop and the surface. This results in a much reduced heat transfer compared to lower surface temperatures, which in turn influences the spray/wall interaction and its outcome. The considered range of T_{Wall} should include these effects and the heating of the target is strong enough to prevent significant spray cooling of the target during the short injections. Therefore, a possible explanation of the negligible dependence on T_{Wall} points to drop/drop interactions which outweigh the influences due to a changed heat transfer.

Surface coverage. The influence of a different surface coverage is exemplarily shown in figures 15-17. Results from a dry target at T_{Wall} = 100°C with an injection pressure p_{Inj} = 50 bar and relative injector position 1, see figure 2, are compared to those on a film-covered target under the same conditions. The two film depths correspond to the different volume fluxes $\dot{Q}_1$ and $\dot{Q}_2$ and are calculated with the central θ –value of the considered θ-class.

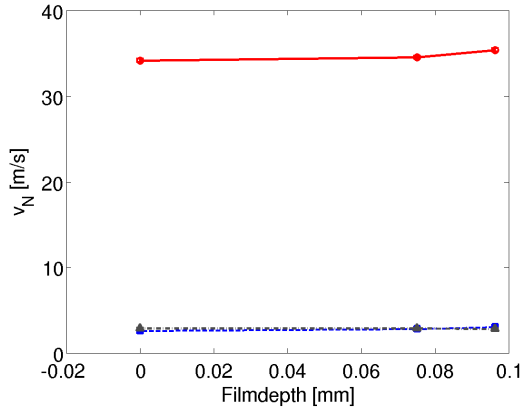

Fig.15: Dependence of wall normal velocity components v_N on film depth for T_{Wall} = 100°C, p_{Inj} = 50 bar and relative position 1 between injector and target. Legend as in figure 12.

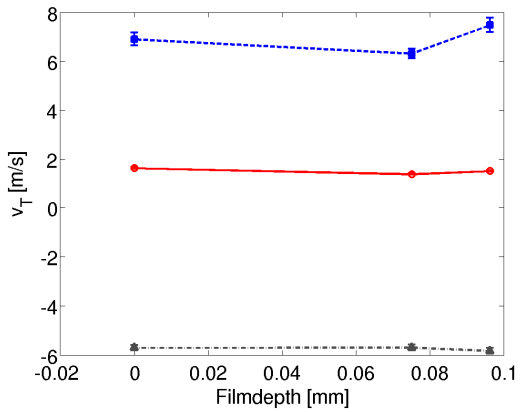

Fig.16: Dependence of wall tangential velocity components v_T on film depth for T_{Wall} = 100°C, p_{Inj} = 50 bar and relative position 1 between injector and target. Legend as in figure 12.

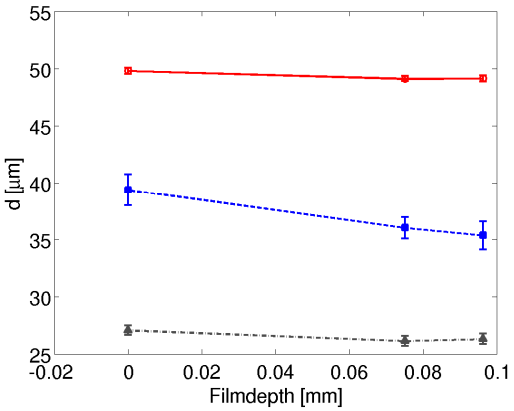

Fig.17: Average drop diameter d in dependence on the film depth for T_{Wall} = 100°C, p_{Inj} = 50 bar and relative position 1 between injector and target. Legend as in figure 12.

Although only two different values of the filmdepth are measured, the results indicate, that also the influence of an externally applied oil film is not decisive. Again, this leads to the conclusion that drop/drop interactions dominate the impact. Possibly, the spray displaces the film very quickly. Thereby, the injection duration t_i could play an important role and a smaller value could result in a stronger influence of the filmdepth. To study this assumption, the measured drop data have been analyzed with respect to their relative arrival time: Using Δt_{SOI}, injections can be separated and the first drop measured for an injection sets the timer for this injection to zero. (Note that due to the drag force the first measured drops need not have been the first injected). However, no significant changes in the magnitudes of the measured diameters and velocity components were observed over the relative arrival time. This suggests, that a smaller value of t_i would not have led to significant changes.

COMPARISON TO THE SINGLE DROP IMPACT MODEL OF G. ELSÄSSER

The experimental results indicate a prevailing influence of drop/drop interactions. The model of G. Elsässer, which is currently used in in-cylinder calculations at BMW does not account for such interactions: similar to most existing models, it is based only on single drop impact data. Therefore, it is unlikely that predicted results using this model can agree with the present experimental data. A comparison will be made to test this hypothesis.

Description of G. Elsässer's model. Three different regimes are distinguished: Cold wetting (CW), hot wetting (HW) and hot non-wetting (HNW). To decide which regime prevails, the wall temperature is compared to two regime temperatures T_{pA} and T_{pR} which separate the regimes CW↔HW and HW↔HNW, respectively. In principle, these are the Nukiyama and the Leidenfrost temperature whereby different experimental values are fitted from literature and generalized formulae are developed, which contain the dependence on the ambient pressure and the different material properties of target and spray.

In CW, the impacting drop experiences rebound, spread or splashing depending on its Weber number and the existing film height (film of spray fluid).

In HW, boiling is another possible outcome where secondary drops are reflected rather vertically from the surface. The wall temperature range of the HW regime is quite small: For an n-heptane drop (20°C) on an aluminium wall, it is limited to approximately $T_{pA} \approx 400$ K- $T_{pR} \approx 425$ K.

In contrast to CW and HW, no wall film is allowed to exist in HNW, as it corresponds to wall temperatures above Leidenfrost. Due to kinematics, rebound or breakup in several child droplets are predicted in this regime.

The model is questionable as it is based on single drop data and applied to spray impact. Moreover, data taken under totally different conditions from different groups have been mingled. In addition to that, the model is restricted to dry surfaces and wall films which consist of the same fluid as the spray itself. However, it covers a parameter range which is adapted to engine conditions.

Comparison of model outcome to experimental results. The evaluated experimental data of the primary drops, namely the weighted mean values $v_{N,primary}$ $v_{T,primary}$ and $d_{primary}$ are used as input in the spray/wall interaction model of G. Elsässer at the respective parameter condition. The results are presented as relative values between secondary and primary drops.

In figures 18-20 the variation of T_{Wall} for dry target, p_{Inj} = 50 bar and relative position 1 between injector and target are shown.

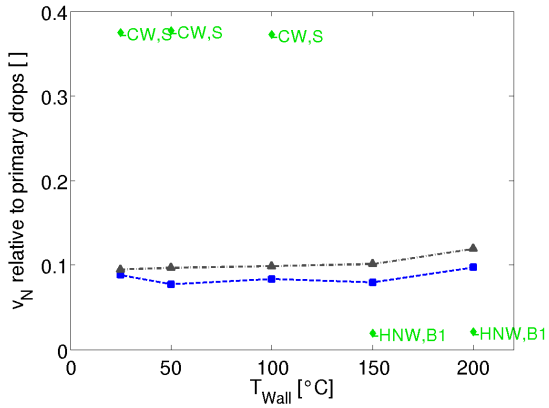

Fig.18: Wall normal velocity components v_N of the secondary drops relative to the primary quantities in dependence on the wall temperature for a dry target with p_{Inj} = 50 bar and relative position 1 between injector and target. Legend for experimental outcome as in figure 12, G.Elsässer's outcome is marked as discrete points: CW,S means splashing in the cold wetting regime, HNW,B1 means boiling in the hot non wetting regime.

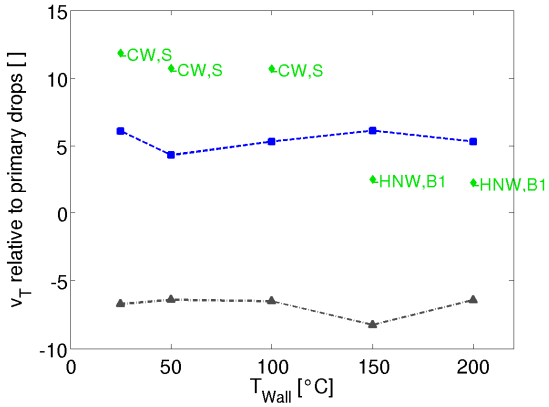

Fig.19: Wall tangential velocity components v_T of the secondary drops relative to the primary quantities in dependence on the wall temperature for a dry target with p_{Inj} = 50 bar and relative position 1 between injector and target. Legend as in figure 18.

These results confirm the expectation, that results according to G. Elsässer's model are completely different from the experimental observations:

- Only one reflection direction for secondary drops is predicted although the impact happens almost normal: In such a case no single preferred direction should exist.
- The velocity components show a much stronger dependence on T_{Wall} than the experimental data and the reflected diameters are much smaller than measured.

Consequently, G. Elsässer's model is not suitable to describe the impact of a dense spray as it does not take any drop/drop interactions into account.

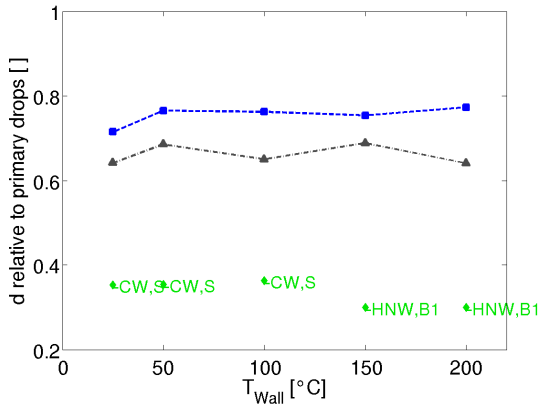

Fig.20: Diameters d of the secondary drops relative to the primary quantities in dependence on the wall temperature for a dry target with p_{Inj} = 50 bar and relative position 1 between injector and target. Legend as in figure 18.

OUTLOOK

Very interesting, but not yet completely treated in the evaluation, is a consideration of the reflected mass compared to the incoming one. It is far from easy as it must carefully account for the discrete distribution of the measuring points.

After finishing the evaluation in the aforementioned manner, a simple model which describes the outcome under the conditions of the experiment is to be developed and introduced in CFD calculations.

In the long term, further experiments are desirable which could study the effect of varying ambient conditions. Moreover, the influence of the surface roughness should be scrutinized. Especially spray impact on coked surfaces, which may store part of the impacting liquid in a porous structure, are of great interest.

NOMENCLATURE

Symbol	Quantity	SI Unit
CW	Cold wetting regime of G.Elsässer's model	
d	Drop diameter	m
d_e	Diameter of the measurement volume	m
g	Absolute value of gravity vector	m^2/s
HW	Hot wetting regime of G.Elsässer's model	
HNW	Hot non-wetting regime of G.Elsässer's model	
$p_{ambient}$	Ambient pressure	N/m^2
p_{Inj}	Injection pressure	N/m^2
$\dot{Q}$	Volume flux of film fluid (oil)	m^2/s
R_a	Average roughness value	m
R_T	Target radius	m
T_{pA}	Temperature separating cold wetting and hot wetting regime in G.Elsässer's model.	K
T_{pR}	Temperature separating hot wetting and hot-non wetting regime in G.Elsässer's model.	K
T_{Wall}	Wall temperature (=film temperature in cases of an applied film)	K
U1, V1	Measured velocity components	m/s
U2, V2	Velocity components adapted to spray wall impact geometry	m/s
v_N, v_T	Velocity components after final transformations	m/s
δ	Film depth	m
ν	Kinematic viscosity	m^2/s
θ	Azimuthal angle on the target hemisphere	deg
θ_0	Mean impact point of the spray cone on the target (calculated due to adjustment).	deg
θ_{Con}	Wall contact point of a drop	deg
$\Delta\theta_{Con}$	Uncertainty of θ_{Con}	deg

REFERENCES

[1] G. E. Cossali, M. Marengo, and M. Santini, Single-drop empirical models for spray impact on solid walls: A review, *Atomization Sprays* vol. 15, 699, 2005.

[2] A. Yarin, Drop impact dynamics: Splashing, spreading, receding, bouncing, …, *Annu. Rev. Fluid Mech.* vol. 38, 159, 2006.

[3] D. Sivakumar, C. Tropea, Splashing impact of a spray onto a liquid film, *Phy. Fluids*, vol. 14, L85, 2003.

[4] C. Tropea and I. V. Roisman, Modelling of spray impact on solid surfaces, *Atomization Sprays* vol. 10, 387, 2000.

[5] I.V. Roisman, K. Horvat, C. Tropea, Spray impact: rim transverse instability initiating fingering and splash, and description of a secondary spray, *Phys. Fluids* vol. 18, 102104, 2006.

[6] G. Elsässer, Experimentelle Untersuchung und Numerische Modellierung der freien Kraftstoffstrahlausbreitung und Wandinteraktion unter motorischen Randbedingungen, Dissertation, Fakultät für Maschinenbau, Universität Karlsruhe (TH), 2001.

[7] H.-E. Albrecht, M. Borys, N. Damaschke, C. Tropea, *Laser Doppler and Phase Doppler Measurement Techniques*, Springer, Heidelberg, 2003.

[8] I.V. Roisman, C. Tropea, Flux measurements in sprays using phase Doppler techniques, *Atomization Sprays* vol. 11, 667-699, 2001.